Energy Components Based Image Fusion Technique for Both Gray Scale and Color Images

Gaurav Choudhary, Manju

Abstract: In this paper, an image fusion scheme based on Hilbert vibration decomposition (HVD) is proposed. In this proposed technique, the images to be fused are first enhanced and then converted into 1-D signals which are decomposed using the HVD technique into different components called energy components. These energy components are fused by taking the average of corresponding energy components except the last component having least energy. Simulation results of the proposed technique are carried out in MATLAB and its performance is compared with other existing techniques using some commonly used performance metrics. It is seen that the proposed technique gives better visual appearance of the fused image than other existing techniques and the values of the several performance metrics are also better/comparable with other techniques. The simulation results obtained for color images show that the proposed algorithm works well for color images in HSI color space also.

Keywords: Image Fusion; Image Enhancement; Hilbert Vibration Decomposition.

I. INTRODUCTION

Image fusion involves improvement of image resolution using multiple images which are either partially focused or obtained from different sources [1]-[22]. The image fusion has applications in many diverse fields such as remote sensing, satellite imaging, computer vision, medical imaging, etc. [1]-[22]. Image fusion has been attempted in spatial as well as transform domains [1]-[22]. The spatial domain methods are based on a local operation and have certain advantages such as ease of implementation and preserving original information from the source images than the transform domain algorithms [3]-[5]. However, these spatial domain algorithms suffer from drawbacks such as reduced contrast, blurring effect etc. [5]. Averaging method, singular value decomposition (SVD) based methods, principal component analysis (PCA) based methods are some of the commonly used methods in spatial domain for image fusion [3], [4]. Transform based methods for image fusion have also been proposed using different transforms, e.g., the pyramid decomposition [6]-[7], discrete wavelet transform (DWT) [8]-[10], stationary wavelet transform (SWT) [11], [12], dual-tree complex wavelet transform (DTCWT) [13], [14], curvelet transform (CVT) [15], [16], contourlet transform (CT) [17], non-subsampled contourlet transform (NSCT) [18], and discrete cosine transform (DCT) based Laplacian pyramid (DCT-LP) [19] etc. These transform domain algorithms have various advantages like high signal to noise ratio,

Gaurav Choudhary, Department of Electronic Engineering, Govt. Polytechnic College Rajsamand, Rajsamand (Rajasthan)-313324, India. E-mail: gauraver.jpr@gmail.com

Manju, Department of Electronic Engineering, Govt. Polytechnic College Neemrana, Daulatsinghpura (Rajasthan)-301709, India. E-mail: manju3650@gmail.com

High quality spectral content etc. [5]-[19]. However, the transform domain algorithms usually generate the fused image results with deterioration due to misregistration of images which is generally not found in spatial domain algorithms [5].

Empirical mode decomposition (EMD) based methods have also been proposed in image fusion techniques [20]-[22] and recently, Hilbert vibration decomposition (HVD) has been introduced as one of the powerful tools in signal processing applications [23], [24] and has attracted attention of researchers [25].

In this paper, the HVD based approach is proposed where the energy components of the sample images are fused. The main motivation for using the HVD in image fusion applications is the fact that as opposed to the EMD approach which provides a time-frequency decomposition of a signal/ image, the HVD decomposes a signal based on the energy of different components of it. Our imaging systems and human vision system is sensitive to not only the frequency content of the scene but also the energy of these components. Hence it will be interesting to investigate the fusion of decomposed images based upon their energy component using the HVD. It is observed through simulation results that the proposed technique gives better visual appearance of the fused image than other existing techniques and the values of the several performance metrics are also better/comparable with other techniques. The simulation results obtained for color images show that the proposed algorithm works well for color images in HSI color space also.

The rest of the paper is organized in the following sections. In section II, a brief review of the HVD has been provided. In section III, we provide the description of the methodology adopted for both the gray scale and color images and finally in section IV, simulation results along with various non-reference performance metrics are given.

II. REVIEW OF HVD

The HVD extracts the mono-components of a signal, called as energy components, using its analytic form [23]. The first energy component corresponds to the highest instantaneous amplitude and is referred to as the dominant component of the signal or the largest energy component [23]. The HVD estimates the largest energy component as an average function of the instantaneous frequency of the decomposition [23].

The HVD technique is an iterative method for extraction of energy components which includes the following steps [23]:

(i) Finding the instantaneous frequency (IF) of the largest energy component.

(ii) Extraction of the corresponding envelope of the largest energy component.

(iii) Finally, subtraction of the largest energy component from the composite signal.

The HVD decomposes a signal $f(t)$ as the sum of different mono-components with slowly varying instantaneous amplitudes and frequencies as given by [23]

$$f(t) = \sum_k a_k(t)\cos\left(\int \omega_k(t)dt\right), \qquad (1)$$

where, $a_k(t)$ and $\omega_k(t)$ are the instantaneous amplitude and the instantaneous frequency respectively of the k th component and these two parameters are determined from the analytic signal representation of the original signal [23]. The other details can be seen in [23]. The "Lena" image and decomposed component images obtained using HVD are shown in Fig. 1.

(a)

(b)

(c)

(d)

(e)
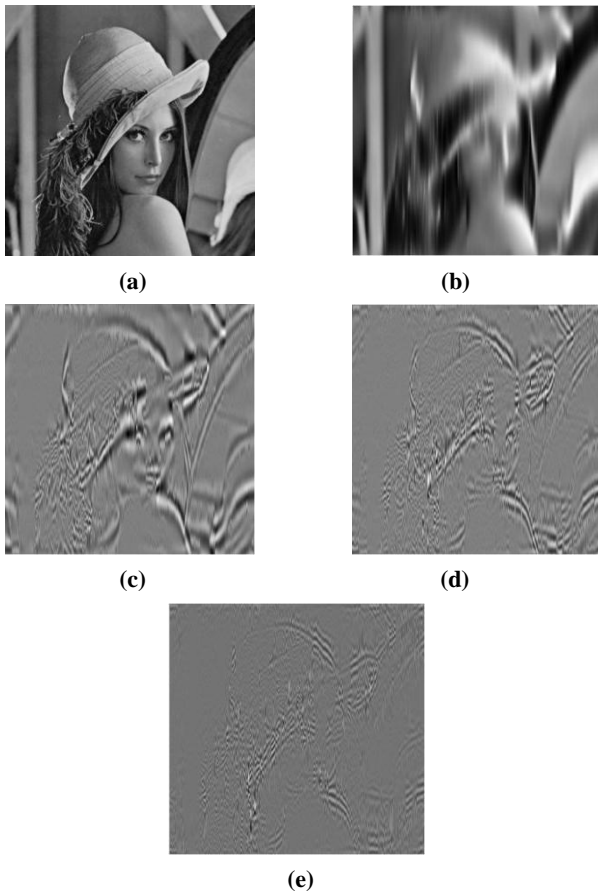
Fig. 1. Energy components for "Lena" sample images based on the decomposition by HVD. (a) Input image. (b) 1st energy component (Highest) (b) 2nd energy component. (c) 3rd energy component. (d) 4th energy component. (e) Least energy component.

III. PROPOSED METHOD FOR IMAGE FUSION

In this section, we present the proposed method for image fusion using the HVD technique. First we consider the fusion of gray scale images.

Step (i): We take the gray scale images of size $L \times M$ to be fused and apply image enhancement technique using minimum mean brightness error bi-histogram equalization (MMBEBHE) method given in [26] for better visual quality and higher contrast. Let the enhanced images be denoted by U and V. Applying image enhancement scheme on these images before decomposition improves visual appearance of the images to be fused.

Step (ii): The enhanced images are then converted to LM dimensional column vectors by column ordering.

Step (iii): Now, the HVD is applied to the column vectors of the enhanced input images. Due to this, the input images are decomposed into a fixed number of energy components.

Step (iv): Then, we fuse the energy component of the decomposed images except the last one (least energy) by averaging rule. The main reason for not fusing the last component of the images to be fused is that this least energy component may correspond to the noise part in the given images. This point has also been observed in the simulation results.

By using the discrete version of the HVD technique in (1), the input images U and V are decomposed as

$$U(n) = \sum_{k=0}^{N-1} a_k^U(n)\cos\left(\sum \omega_k^U(n)\right), \qquad (2)$$

And

$$V(n) = \sum_{k=0}^{N-1} a_k^V(n)\cos\left(\sum \omega_k^V(n)\right). \qquad (3)$$

The fusion is performed by fusing first $N-1$ higher energy components in (2) and (3) and the fused image can be expressed as any one of the following two equations

$$W(n) = \sum_{k=0}^{N-2}\left[\left(a_k^V(n) + a_k^U(n)\right)/2\right]\cos\left(\sum_n \omega_k^V(n)\right)$$

$$+ a_{N-1}^V(n)\cos\left(\sum_n \omega_{N-1}^V(n)\right), \qquad (4)$$

Or

$$W(n) = \sum_{k=0}^{N-2}\left[\left(a_k^V(n) + a_k^U(n)\right)/2\right]\cos\left(\sum_n \omega_k^U(n)\right)$$

$$+ a_{N-1}^U(n)\cos\left(\sum_n \omega_{N-1}^U(n)\right). \qquad (5)$$

Step (v): Finally, the fused column vector W is again converted to 2-D signal, say F, whose size is same as the size of the input image. The block diagram of the method described above is shown in Fig. 2.
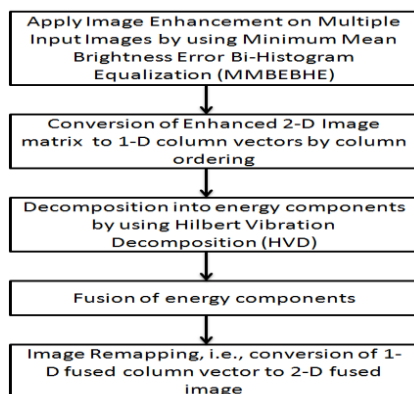
Fig.2.The Block Diagram of the Proposed Image Fusion Scheme for Gray Scale Images.

For the fusion of color images, the source images are first enhanced through a technique which avoids gamut problem [27]. Then images from RGB format are converted into HSI format which are converted into corresponding 1-D vectors. This is done because the fusion results are sensitive and can deteriorate if we directly fuse/modify the RGB color components. The HVD is then applied on each of the H, S, I components separately and the fusion rule is applied on the corresponding components of decomposed vectors. These fused vectors are converted into 2-D image and the fused image is obtained by converting HSI image back to RGB color space. The block diagram of the method for color images is shown in Fig. 3.
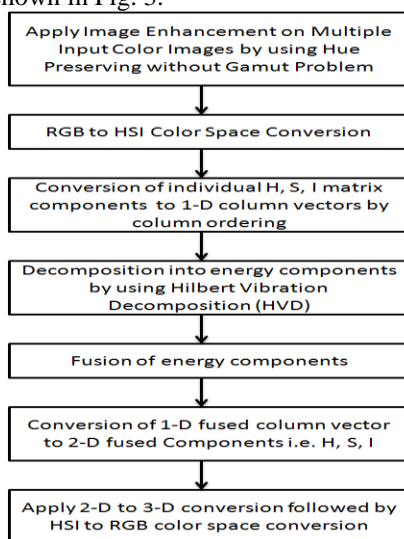
Fig.3.The Block Diagram of the Proposed Image Fusion Scheme for Color Images.

IV. EXPERIMENTS AND ANALYSIS

In this section we provide the simulation results of the proposed technique carried out in MATLAB. The details of testing data and various fusion metrics are given below.

4.1. Testing Data and Results

The proposed method for gray scale images has been implemented in MATLAB on three sets of images: "Watch", "PET & MRI", and "Lena" images which are shown in Fig. 4 to Fig. 6. The number of energy components in which the input images are decomposed is selected as 6 by experiments and the fused image obtained for different kinds of input images as shown in Fig. 4 to Fig. 6 are compared with some already existing image fusion techniques such as averaging method in spatial domain [3], [4], discrete cosine transform based Laplacian pyramid method [19],

and stationary wavelet transform based method [11], [12]. It is clearly seen from different figures that the fused image obtained from the proposed method give better visual appearance as compared to the other existing image fusion techniques. The results for color images are shown in Fig. 7 and Fig. 8 which clearly show that the proposed algorithm works well for color images in HSI color space.
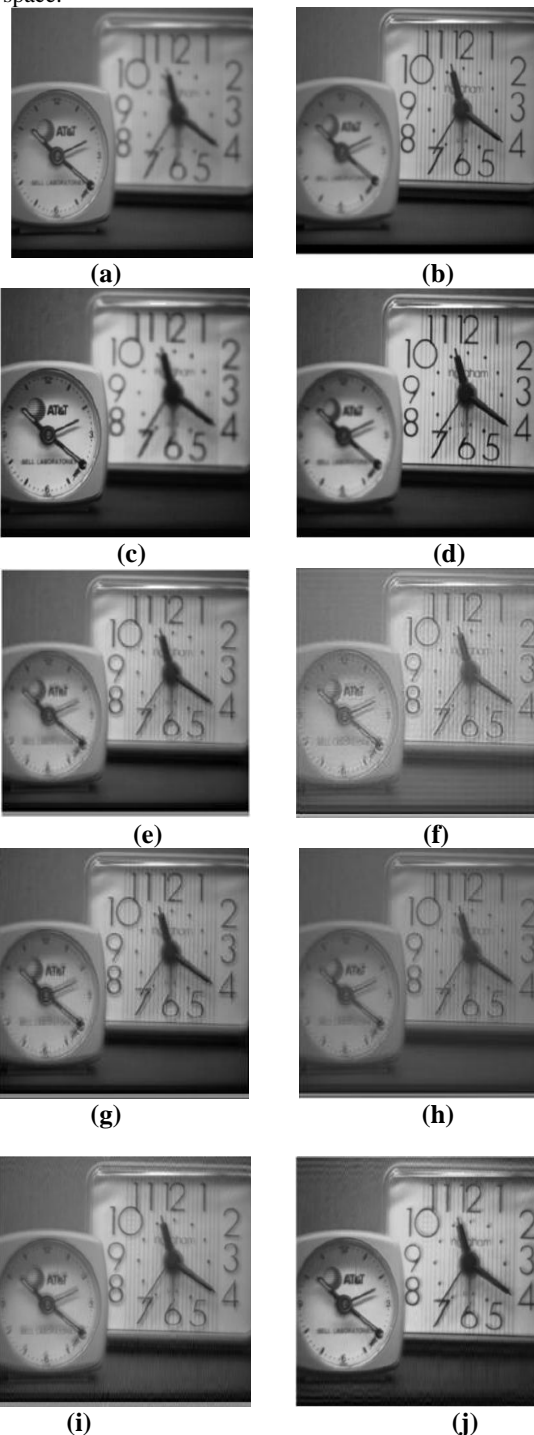
Fig. 4. Fusion results for "Watch"' sample images. (a) 1st input image. (b) 2nd input image. (c) Enhanced version of 1st input image. (d) Enhanced version of 2nd input image. (e) Averaging method in spatial domain. (f) DCT-LP method. (g) SWT-Level 1 method. (h) SWT-Level 2 method. (i) Proposed method (without enhancement). (j) Proposed method (with enhancement).
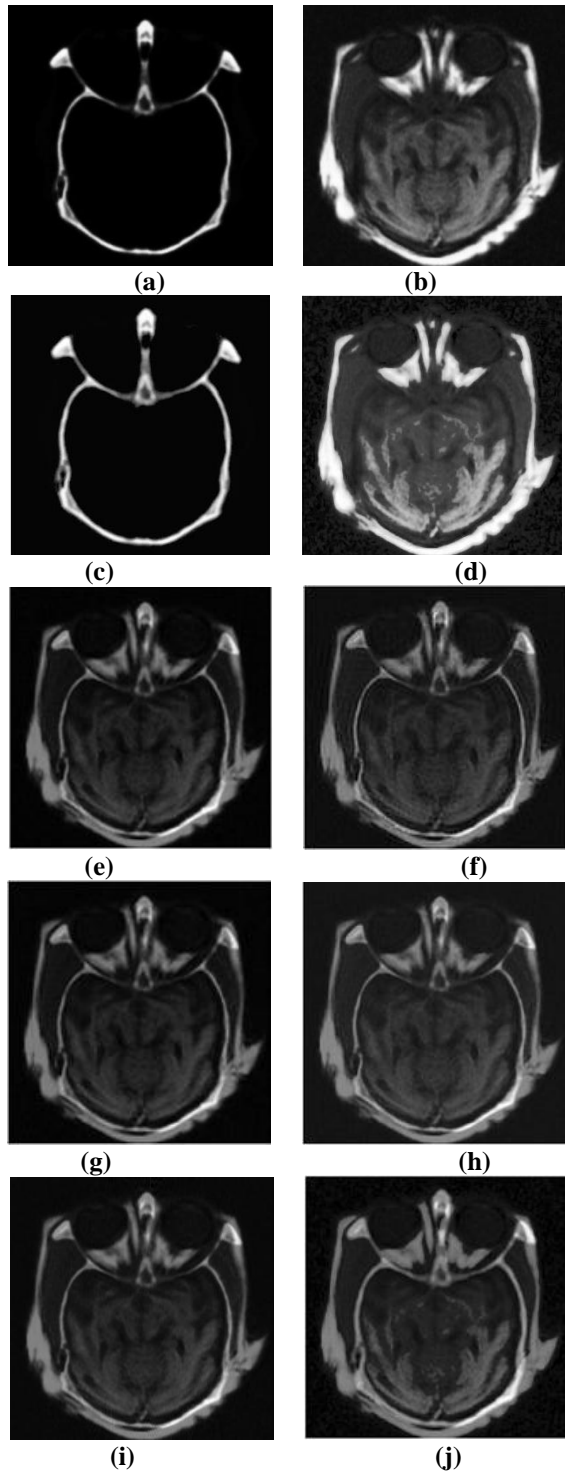
Fig. 5.Fusion results for "PET and MRI"' sample images. (a) 1st input image. (b) 2nd input image. (c) Enhanced version of 1st input image. (d) Enhanced version of 2nd input image. (e) Averaging method in spatial domain. (f) DCT-LP method. (g) SWT-Level 1 method. (h) SWT-Level 2 method. (i) Proposed method (without enhancement). (j) Proposed method (with enhancement).
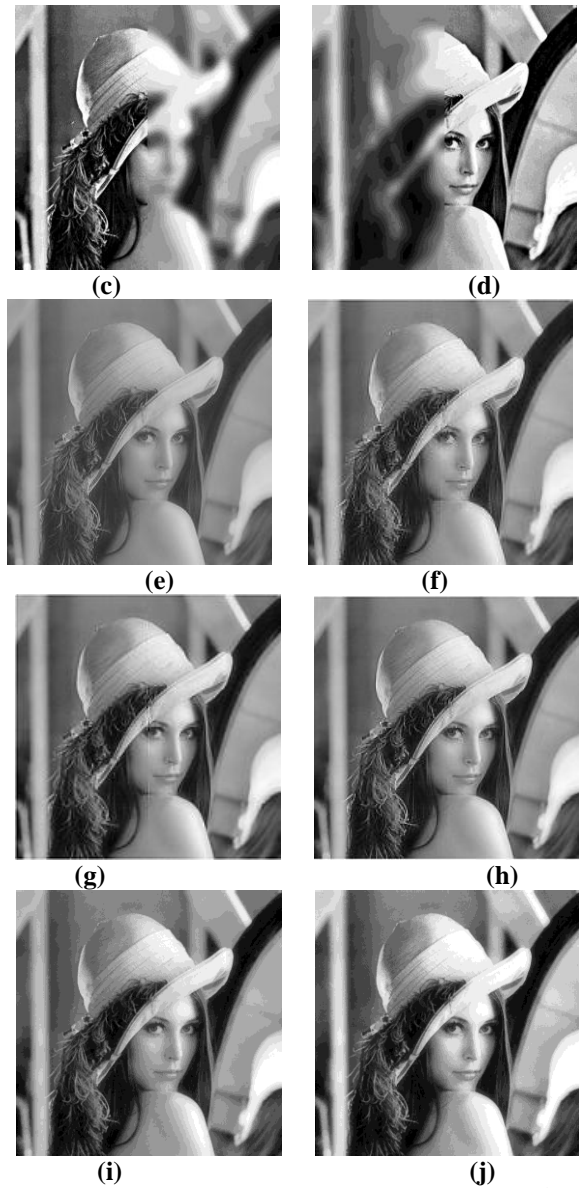
Fig. 6. Fusion results for "Lena"' sample images. (a) 1st input image. (b) 2nd input image. (c) Enhanced version of 1st input image. (d) Enhanced version of 2nd input image. (e) Averaging method in spatial domain. (f) DCT-LP method. (g) SWT-Level 1 method. (h) SWT-Level 2 method. (i) Proposed method (without enhancement). (j) Proposed method (with enhancement).

(c)   **(d)**

Fig. 7. Fusion results for color sample images. (a) 1st input image. (b) 2nd input image. (c) Proposed method (without enhancement). (d) Proposed method (with enhancement).
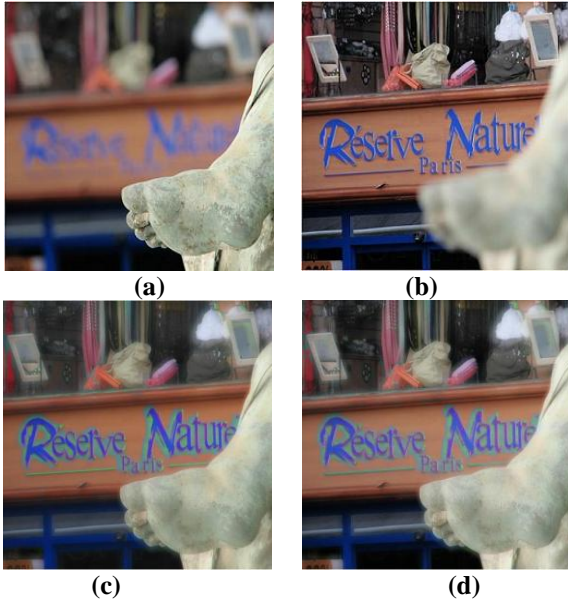
(a)   **(b)**

(c)   **(d)**

Fig. 8. Fusion results for color sample images. (a) 1st input image. (b) 2nd input image. (c) Proposed method (without enhancement). (d) Proposed method (with enhancement).

4.2. Metrics for Performance Evaluation

The brief description of various non-reference performance metrics such as mutual information (MI), information entropy (H), $Q^{UV/F}$, and standard deviation (σ) is given below for ready reference.

4.2.1. Mutual Information (MI): The mutual information (MI) is a measure of random variables' mutual dependence, by measuring the distance between the joint distribution $p_{XY}(x,y)$ and the distribution associated with the case of the complete independence $p_X(x) p_Y(y)$, by means of relative entropy in [28] as

$$I_{XY} = \sum_{x,y} p_{XY}(x,y) \log_2 \frac{p_{XY}(x,y)}{p_X(x) p_Y(y)}, \qquad (6)$$

where, X and Y are the two discrete random variables. Now, consider two source images U and V, and the fused image F, the amount of information that F contains about U and V is calculated in [28] as

$$I_{FU} = \sum_{f,u} p_{FU}(f,u) \log_2 \frac{p_{FU}(f,u)}{p_F(f) p_U(u)}, \qquad (7)$$

and

$$I_{FV} = \sum_{f,v} p_{FV}(f,v) \log_2 \frac{p_{FV}(f,v)}{p_F(f) p_B(v)}. \qquad (8)$$

Consequently, the image fusion performance measure can be calculated as [28]

$$MI = I_{FU} + I_{FV}. \qquad (9)$$

4.2.2. Information Entropy (H): The entropy $H(k)$ of a discrete random variable k is defined as [28]

$$H(k) = -\sum_{i=0}^{L-1} p_F(i) \log_2 p_F(i), \qquad (10)$$

where, k, p_F, and L are the gray-level index, the normalized histogram of the fused image, and the number of bins in the histogram, respectively [28].

4.2.3 Xydeas and Petrovic metric: Xydeas and Petrovic proposed an objective performance metric, which basically measures the relative amount of edge information that is transferred from the source images A and B into the fused image, F [28], [29]. This method uses a Sobel edge detectorto calculate the strength $g(m,n)$ and orientation $\alpha(m,n)$ information together at each pixel in both the source and fused images. The relative strength and orientation values of a source image U, with respect to the fused image F, are defined in [28] as

$$G_{m,n}^{UF} = \frac{g_F(m,n)}{g_U(m,n)}; \; g_U(m,n) > g_F(m,n)$$

$$\frac{g_U(m,n)}{g_F(m,n)}; \; otherwise. \qquad (11)$$

$$A_{m,n}^{UF} = 1 - \frac{|\alpha_U(m,n) - \alpha_F(m,n)|}{\pi/2}. \qquad (12)$$

Edge information preservation values are calculated as [28]

$$Q_{m,n}^{UF} = \Gamma_g \Gamma_\alpha \left(1 + e^{K_g \left(G_{m,n}^{UF} - \sigma_g\right)}\right)^{-1} \left(1 + e^{K_\alpha \left(A_{m,n}^{UF} - \sigma_\alpha\right)}\right)^{-1}, \qquad (13)$$

where, the constants Γ_g, K_g, σ_g, and Γ_α, K_α, σ_α determine the exact shape of the sigmoid function used to form the edge strength and orientation [28]. Having $Q_{m,n}^{UF}$ and $Q_{m,n}^{VF}$ for two $L \times M$ source images, a normalized weighted performance metric is obtained in [28] as.

$$Q^{UV/F} = \frac{\sum_{m=1}^{M} \sum_{n=1}^{N} Q_{m,n}^{UF} w_{m,n}^{UF} + Q_{m,n}^{VF} w_{m,n}^{VF}}{\sum_{m=1}^{M} \sum_{n=1}^{N} w_{m,n}^{UF} + w_{m,n}^{VF}}, \qquad (14)$$

where, $Q_{m,n}^{UF}$ and $Q_{m,n}^{VF}$ are the edge preservation values and are weighted by the values of $w_{m,n}^{UF}$ and $w_{m,n}^{VF}$, which are defined as $w_{m,n}^{UF} = \left[g_U(m,n)\right]^L$ and $w_{m,n}^{VF} = \left[g_U(m,n)\right]^L$, where L is a constant and $0 \le Q^{UV/F} \le 1$ [28].

4.2.4 Standard deviation (σ): This metric is more efficient in absence of noise. It basically measures the contrast in the fused image. An image with high contrast would have high standard deviation [28]. The standard deviation as a measure of contrast of the fused image is calculated as [28]

$$\sigma = \sqrt{\sum_{i=0}^{L-1} (i - i') p_F(i)}, \qquad (15)$$

and

$$i' = \sum_{i=0}^{L-1} i \, p_F(i). \qquad (16)$$

4.3. Performance Evaluation and Analysis

As explained in the above section 4.2, the non-reference performance metrics are calculated for different fused images using the proposed method. The results for "Watch" sample image are shown in Table 1 and compared with other existing methods. Similarly, for "PET+MRI" image and "Lena" images, the results are given in Table 2 and 3 respectively. From Table 1 to Table 3, it is observed that the entropy (H) and standard deviation (σ) metrics obtained by the proposed image fusion scheme are better than the previously existing techniques in the literature, while other performance metrics such as mutual information and $Q^{UV/F}$ etc. are comparable with the results of other techniques. The improved results using the proposed technique may be attributed to the decomposition strategy exploited by the HVD technique based on energy of the constituting components of the signals.

Table 1. Comparison of Methods using Performance Evaluation Metrics for Fig. 4.

Watch	MI(F, U)	MI (F, V)	Entropy	Q^UV/F	σ
Proposed (with MMBEHE)	2.8417	2.1246	7.7322	0.3230	59.7498
Proposed (without MMBEHE)	2.5398	2.6902	7.4110	0.4329	44.8809
Averaging (Spatial Domain)	2.8693	2.9621	7.3736	0.5032	44.6292
DCT-LP	2.2954	2.6166	7.4500	0.5308	46.0964
SWT (Level 1)	2.7483	2.9560	7.4319	0.5649	45.6790
SWT (Level 2)	2.6942	2.9557	7.4399	0.5777	45.9242

Table 2. Comparison of Methods using Performance Evaluation Metrics for Fig. 5.

PET+MRI	MI (F, U)	MI (F, V)	Entropy	Q^UV/F	σ
Proposed (with MMBEHE)	0.5346	2.3921	6.7659	0.3207	41.3813
Proposed (without MMBEHE)	0.5274	3.3248	6.0999	0.4311	35.7827
Averaging (Spatial Domain)	0.5885	4.4678	6.0158	0.4363	35.5772
DCT-LP	0.5249	2.5238	6.2238	0.4641	36.0867
SWT (Level 1)	0.5820	3.8613	6.0949	0.4654	35.6873
SWT (Level 2)	0.5774	3.7004	6.1024	0.4813	35.6873

Table 3. Comparison of Methods using Performance Evaluation Metrics for Fig. 6.

Lena	MI (F, U)	MI (F, V)	Entropy	Q^UV/F	σ
Proposed (with MMBEHE)	2.3006	2.3000	7.8807	0.5746	69.6461
Proposed (without MMBEHE)	2.3224	2.3191	7.2646	0.5117	41.9824
Averaging (Spatial Domain)	2.3349	2.3446	7.2604	0.5106	41.8401
DCT-LP	2.2892	2.2026	7.3000	0.6132	42.4378
SWT (Level 1)	2.3271	2.2850	7.2773	0.5917	42.0446
SWT (Level 2)	2.3265	2.2723	7.2811	0.6103	42.1284

V. CONCLUSION AND FUTURE WORK

In this work, a method for image fusion using the HVD is proposed. The simulation results obtained with the proposed method give better visual appearance of the fused image than other existing techniques. The values of the several performance metrics of the fused images using the proposed technique are also better/comparable with other techniques existing in the literature. The simulation results obtained for color images show that the proposed algorithm works well for color images in HSI color space also. However, the proposed method is based on 1-D HVD and the use of 2-D HVD based fusion is yet to be explored.

REFERENCES

1. Li, Shutao, Bin Yang, and Jianwen Hu. "Performance comparison of different multi-resolution transforms for image fusion." Information Fusion, vol.12, no. 2, pp. 74-84, 2011.
2. Pohl, Christine, and John van Genderen. "Structuring contemporary remote sensing image fusion." International Journal of Image and Data Fusion, vol. 6, no. 1, pp. 3-21, 2015.
3. Zhijun Wang, "A comparative Analysis of Image fusion Methods." IEEE Trans. on GeoscienceAnd Remote SenSing,vol. 43, pp. 1391-1402, 2005.
4. T. M. Tu, S.c. Su, H.C. Shyu, and P. S. Huang, "A new look at HIS likeimage fusion methods, " Information Fusion J, vol. 2, pp. 177-186, 2001.

5. Bai, Xiangzhi, Yu Zhang, Fugen Zhou, and Bindang Xue. "Quadtree-based multi-focus image fusion using a weighted focus-measure." Information Fusion, vol. 22, pp. 105-118, 2015.
6. Toet, Alexander. "Image fusion by a ratio of low-pass pyramid." Pattern Recognition Letters, vol. 9, no. 4, pp. 245-253, 1989.
7. Liu, Zheng, Kazuhiko Tsukada, Koichi Hanasaki, Yeong-Khing Ho, and Y. P. Dai. "Image fusion by using steerable pyramid." Pattern Recognition Letters, vol. 22, no. 9, pp. 929-939, 2001.
8. Li, Hui, B. S. Manjunath, and Sanjit K. Mitra. "Multisensor image fusion using the wavelet transform." Graphical models and image processing, vol. 57, no. 3, pp. 235-245, 1995.
9. Zhang, Zhong, and Rick S. Blum. "A categorization of multiscale-decomposition-based image fusion schemes with a performance study for a digital camera application." IEEE Proceedings, vol. 87, no. 8, pp. 1315-1326, 1999.
10. Pajares, Gonzalo, and Jesus Manuel De La Cruz. "A wavelet-based image fusion tutorial." Pattern recognition, vol. 37, no. 9,pp. 1855-1872, 2004.
11. Unser, Michael. "Texture classification and segmentation using wavelet frames." IEEE Trans. on Image Processing, vol. 4, no. 11, pp. 1549-1560, 1995.
12. Li, Shutao, James T. Kwok, and Yaonan Wang. "Using the discrete wavelet frame transform to merge Landsat TM and SPOT panchromatic images."Information Fusion, vol. 3, no. 1, pp. 17-23, 2002.
13. Forster, Brigitte, Dimitri Van De Ville, Jesse Berent, Daniel Sage, and Michael Unser. "Complex wavelets for extended depth-of-field: A new method for the fusion of multichannel microscopy images." Microscopy Research and technique, vol. 65, no. 1-2, pp. 33-42, 2004.
14. Ray, Lee A., and Reza R. Adhami. "Dual tree discrete wavelet transform with application to image fusion." IEEE Proceeding of the Thirty-Eighth Southeastern Symposium on System Theory, pp. 430-433, 2006.
15. Nencini, Filippo, Andrea Garzelli, Stefano Baronti, and Luciano Alparone. "Remote sensing image fusion using the curvelet transform." Information Fusion, vol. 8, no. 2, pp. 143-156, 2007.
16. Tessens, Linda, Alessandro Ledda, Aleksandra Pizurica, and Wilfried Philips. "Extending the depth of field in microscopy through curvelet-based frequency-adaptive image fusion.", 2007. ICASSP 2007. IEEE International Conference on Acoustics, Speech and Signal Processing, vol. 1, pp. I-861, 2007.
17. Do, Minh N., and Martin Vetterli. "The contourlet transform: an efficient directional multiresolution image representation." IEEE Trans. on Image Processing, vol. 14, no. 12, pp. 2091-2106, 2005.
18. Da Cunha, Arthur L., Jianping Zhou, and Minh N. Do. "The nonsubsampled contourlet transform: theory, design, and applications." IEEE Trans. on Image Processing, vol. 15, no. 10, pp. 3089-3101, 2006.
19. Naidu, V. P. S., and Bindu Elias. "A Novel Image Fusion Technique using DCT based Laplacian Pyramid." International Journal of Inventive Engineering and Sciences (IJIES), pp. 2319-9598, 2013.
20. Shaohui, Renhua Zhang, Hongbo Su, et al. "SAR and multispectral image fusion using generalized IHS transform based on a trous wavelet and EMD decompositions."IEEE Sensors Journal, vol. 10, no. 3, pp. 737-745, 2010.
21. Dong, Weihua, Xian'en Li, Xiangguo Lin, et al. "A Bidimensional Empirical Mode Decomposition Method for Fusion of Multispectral and Panchromatic Remote Sensing Images." Remote Sensing, vol. 6, no. 9, pp. 8446-8467, 2014.
22. Ehsan, Shoaib, Syed Muhammad Umer Abdullah, et al. "Multi-Scale Pixel-Based Image Fusion Using Multivariate Empirical Mode Decomposition."Sensors, vol. 15, no. 5, pp. 10923-10947, 2015.
23. Feldman, Michael. "Time-varying vibration decomposition and analysis based on the Hilbert transform." Journal of Sound and Vibration, vol. 295, no. 3, pp. 518-530, 2006.
24. Feldman, Michael. "Hilbert transform in vibration analysis." Mechanical Systems and Signal Processing, vol. 25, no. 3, pp. 735-802, 2011.
25. Sharma, H., and K. K. Sharma. "Baseline wander removal of ECG signals using Hilbert vibration decomposition." Electronics Letters, vol.51, no. 6, pp. 447-449, 2015.
26. Chen, Soong-Der, and Abd Rahman Ramli. "Minimum mean brightness error bi-histogram equalization in contrast enhancement." IEEE Trans. on Consumer Electronics, vol. 49, no. 4,pp. 1310-1319, 2003.
27. Naik, Sarif Kumar, and C. A. Murthy. "Hue-preserving color image enhancement without gamut problem." IEEE Trans. on Image Processing, vol. 12, no. 12, pp. 1591-1598, 2003.
28. Haghighat, Mohammad Bagher Akbari, Ali Aghagolzadeh, and Hadi Seyedarabi. "A non-reference image fusion metric based on mutual information of image features." Computers & Electrical Engineering 37, vol. 5, pp. 744-756, 2011.
29. Xydeas, C. S., and V. Petrović. "Objective image fusion performance measure." Electronics Letters, vol. 36, no. 4, pp. 308-309, 2000.